

## Location and motion of sources of Jupiter's magnetospheric/auroral decameter emissions

Observation request of the Planets-Exoplanets Working Group (PEWG) on behalf of LOFAR's Transients Key Project (TKP), and LOFAR's Long Baselines working group, under the umbrella of the LRA12A004 Transients proposal (Call A). P.I.s : O. Wucknitz (Long Baselines expertise) & P. Zarka (scientific expertise on the target).

### Abstract

We will perform observations of Jupiter's decameter emission in the 10–40 MHz range using LOFAR long baselines, in order to determine with arcsec accuracy the source locations and motions along Jovian magnetic field lines. This determination will confirm (or falsify!) the theoretical frame of planetary (and exoplanetary) auroral radio emissions, and provide new breakthrough on the Jovian magnetosphere and radio emissions. We will analyze our observations in « expert » mode independently of the CEP2 cluster, and in this way prepare the exploitation of future special modes of LOFAR Long Baselines observations.

### Astrophysical goals

Jupiter is one of the most intense radio-sources below 40 MHz, with the flux density received at Earth commonly reaching  $10^{-6}$ – $10^{-7}$  Jy (Figure 1) [Zarka, 2004a]. Its decameter-wave (DAM) emission is produced by electrons energized to a few keV moving along high-latitude field lines in Jupiter's magnetosphere. Emission is generated at the local electron cyclotron frequency ( $f_{ce} = eB/2\pi m_e$  of the location) where the electrons lie or pass at a given time, and thus high frequencies are produced close to the planet (up to 40 MHz near Jupiter's surface) whereas low frequencies are produced a few tenths to a few Jovian radii ( $1 R_J = 71400$  km) above the surface. DAM is highly elliptically polarized, in the Right-Hand sense (relative to the  $\mathbf{k}$  wave vector) from the northern hemisphere and in the Left-Hand sense from the southern hemisphere, consistent with emission of RH polarized waves with respect to the magnetic field in the source and with the orientation of the Jovian internal field (northern magnetic pole in the northern rotational hemisphere).

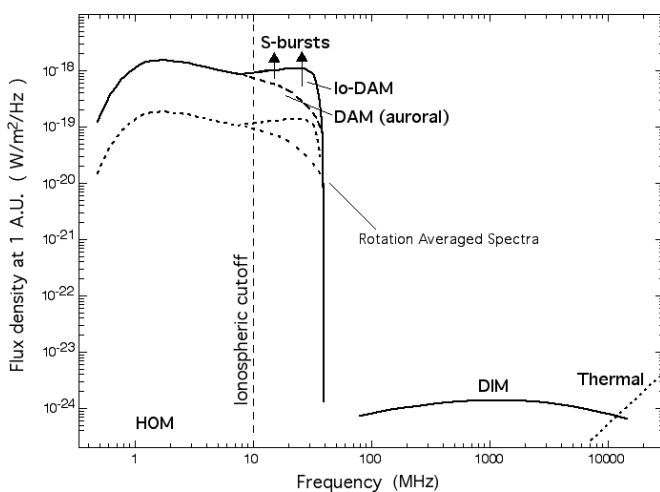


Figure 1 : Jupiter's radio spectrum at Earth's distance. DIM is the decimeter synchrotron emission from the radiation belts. DAM emission includes auroral-DAM (dashed), which extends down to the hectometer range, and Io-DAM (solid - part of which consists of impulsive bursts (S-bursts)). The Earth's ionospheric cut-off lies on the average at about 10 MHz. The sharp cut-off at 40 MHz corresponds to the maximum of  $f_{ce}$  at the planetary surface. Dotted lines show the average spectrum, whereas solid/dashed lines are peak intensities.

The generation mechanism of DAM, similar to that of all dominant planetary magnetospheric radio emissions (including the Earth's Auroral Kilometric Radiation), has been identified and extensively studied. It is the ubiquitous Cyclotron-Maser Instability (CMI – Zarka, 2004b ; Treumann, 2006), a nonthermal coherent process involving resonance between the electron's perpendicular (cyclotron) motion around the magnetic field lines and the electric field of circular/elliptical radio waves. Its predictions match all observable parameters, and thus this mechanism provided a reliable theoretical frame that permits to use radio emissions as a diagnostic of magnetospheric structure and dynamics, magnetosphere-ionosphere coupling strength, and interaction magnetosphere-satellites and magnetosphere-solar wind at all magnetized planets (Zarka, 1998). But only Jupiter has an intense enough magnetic field for emitting at  $f_{ce}$  up to 40 MHz, whereas the surface  $f_{ce}$  does not exceed 2 MHz for all other magnetized planets, meaning that their emissions are not observable from the ground.

Two distinct radio components superimpose in the DAM range, with similar physical characteristics but different occurrences (Zarka, 2004a) : one – called Io-DAM – is related to the Jovian satellite Io, in the sense that it is detected only for two specific ranges of the Io-Jupiter-observer angle, when Io is close to the East or West limb of the planet. This is explained by the fact that Io is a source of accelerated electrons (via Alfvén waves and magnetic-

field-aligned currents excited by the Io-magnetosphere interaction), and that DAM emission is very anisotropic, being beamed at large angles from the magnetic field line along which emission occurs (the beaming at each frequency is along the walls of a widely open hollow cone centered on the source magnetic field). The other DAM component – called non-Io-DAM – is related to the auroral oval, at higher magnetic latitude than the former one (Figure 2). Its occurrence depends on the Jovian longitude of the observer, but not on the position of Io.

Besides having different occurrences, these components also differ by the morphology of the emission in the time-frequency plane, in which DAM has a very rich morphology : it is structured in « storms » (period of strong emission lasting for tens of minutes to hours), which can themselves consist of « arcs » of emission and shorter « bursts » down to the second or even millisecond timescale (Figure 2). These bursts are instantaneously narrowband, and they drift – most often negatively – in frequency, which has been interpreted as the upward motion of source electron bunches along high latitude magnetic field line such as the one linking Io to Jupiter. Detailed analysis of these drifting bursts has even revealed electric potential jumps aligned with the magnetic field, themselves in motion (Hess et al., 2007, 2009). Various fringes due to Faraday rotation (during the traversal of the plasma torus surrounding Io, or of the Earth’s ionosphere) or other unidentified causes (satellites...) superimpose to form the complex time-frequency structure of Jovian DAM (e.g. Figure 4).

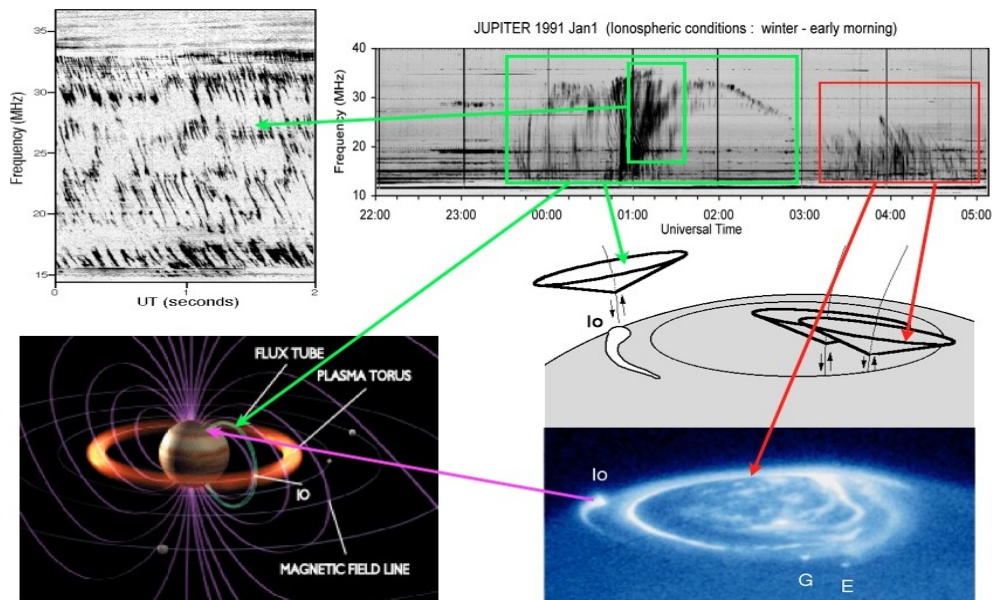


Figure 2 : (top right) Dynamic spectrum of Jovian DAM showing arcs (from 01:00 to 03:00, and 03:30 and 05:00) and fringes (e.g. From 00:30 to 01:30, around the start of the first arc). Green-boxed emission comes from the Io-Jupiter field line (bottom left). Red-boxed emission comes from above the main aurora (bottom right). Radio emission cones are emitted above UV auroral spots. Part of Io-DAM consists of short drifting bursts (top left).

The DAM spectral range observable from the ground (10–40 MHz) corresponds to an altitude range from ~0 to ~0.6 RJ above the surface, i.e. an angular extent on the sky ~13 arcsec (Jupiter’s average diameter, at a typical distance of 4.2 AU from Earth near Jupiter’s opposition, is 44 arcsec). No imaging study of DAM sources was ever performed, except VLBI visibility amplitude measurements in the 1970’s that put limits on the instantaneous source size (Dulk, 1970), repeated in 2005 with LOFAR’s initial test station and the Nançay Decameter Array (Nigl et al., 2007), and spacecraft Goniopolarimetric studies (with Ulysses, below 1 MHz – Ladreiter et al., 1994), a kind of astrometric technique that allowed us to deduce source locations consistent with the local cyclotron frequency. As a consequence, all the emission characteristics (source position, beaming angle at emission...) and the generation scenarios deduced from them only rely on indirect conclusions drawn from dynamic spectra (t-f images) in intensity and polarization.

LOFAR's long (international) baselines provide an angular resolution of 1.5 to 6 arcsec in the 10–40 MHz range. Through imaging, or even just absolute astrometry of Jovian DAM sources, we will measure directly for the first time the position (and motion) of these sources. This will both confirm and solidly ground all past studies of planetary auroral radio emissions (as well as their application to exoplanets), but will also provide new breakthroughs on the Jovian magnetosphere and radio emissions (Zarka, 2004a) :

- (1) an improved mapping of the surface planetary magnetic field, via imaging of instantaneous cyclotron sources of highest frequency (ca. 40 MHz);
- (2) measurements of the beaming angle of the radiation relative to the local magnetic field, as a function of frequency;
- (3) detailed information on the Io–Jupiter electrodynamic interaction, in particular the lead angle between the Io flux tube and the instantaneously radio emitting field line;
- (4) direct information on the origin of the sporadic drifting decameter millisecond bursts, thought to be electron bunches propagating along magnetic field lines, and possibly revealing electric potential drops along these field lines;
- (5) direct observation of DAM emission possibly related to the Ganymede–Jupiter, Europa–Jupiter and/or Callisto–Jupiter interactions, and their energetics;
- (6) information on the magnetospheric dynamics, via correlation of radio images with ultraviolet and infrared images of the aurora as well as of the Galilean satellite footprints, and study of their temporal variations;
- (7) an improved mapping of the Jovian plasma environment (especially the Io torus) via the propagation effects that it induces on the radio waves propagating through it (Faraday rotation, diffraction fringes, etc.);
- (8) possibly on the long-term a better accuracy in the determination of Jupiter’s rotation period.

Topic (4) will require not only accurate astrometry/imaging, but also that images can be formed at intervals of a few tens of msec. This is made possible by the very high flux density of Jovian DAM, although not with the standard imaging pipeline, but rather with the specific methods and software developed by the Long Baselines WG.

DAM is intrinsically sporadic and due to its beaming anisotropy that makes any given source observable only for a short time (Figure 2). Whereas auroral non-Io-DAM activity/intensity is very difficult to predict (it is partly controlled by the solar wind pressure and shock arrivals at Jupiter – Hess et al., 2012), Io-DAM is very predictable, with an activity/intensity strictly controlled by the Io-Jupiter-observer geometry (Nigl et al., 2007). Io-DAM emissions occur several times per month for a few tens of minutes to a few hours. Io-DAM emitted from the East (resp. West) limb in the northern hemisphere is called Io-A (resp. Io-B) emission. It is RH polarized. Io-C (resp. Io-D) are LH counterparts from the southern hemisphere (Figure 3a). Io-A and Io-C emissions may occur simultaneously or consecutively, and the same is true for Io-B and Io-D emissions.

We request observations of Io-DAM emissions at times of predicted activity. We have successfully tested during LOFAR’s commissioning phase the reliability of such predictions (Nigl et al., 2007, and tests between LOFAR and Nancay). We would prefer nighttime observations in order to have good observations down to 10 MHz. The beginning of cycle 0 (Dec. 2012) is more favourable to nighttime Jupiter emission (cf. Table 1).

Source positions and motions will be derived by reference to a nearby calibrator, whenever possible. Because source motion is very difficult to distinguish from source wandering due to ionospheric delays and fluctuations, we will in addition select time intervals when 2 sources from opposite hemispheres, with opposite senses of circular/elliptical polarization (LH & RH), can be observed (quasi-)simultaneously. Ionospheric perturbations will cause the same motion for both sources, whereas intrinsic source motions will be in opposite direction in the two hemispheres.

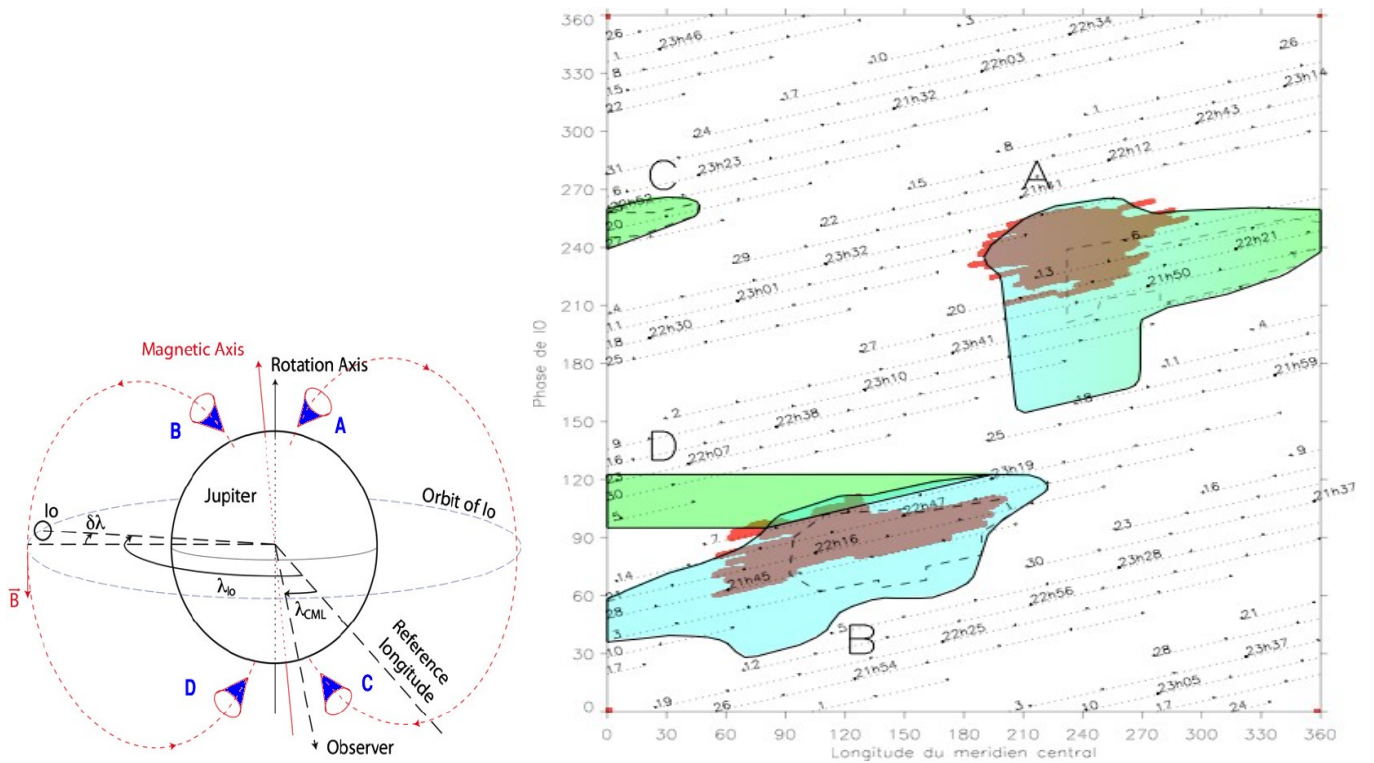


Figure 3 : (a – left) Sketch of the geometry of Io-DAM emissions corresponding to the nomenclature of Io-A, B, C and D sources (from Hess et al., 2010). (b – right) Exploration of the plane Observer's longitude (CML) – Io's phase (i.e. anti-observer/Jupiter/Io angle) in Dec. 2012. Each dotted track represents 8h of observations around Jupiter's transit at meridian. The number on the left of each track (near 1st dot) is the day of month, and that in the middle of each track (near 5th dot) is the time (UT) of meridian transit. RH Io-A & -B emissions are detected when the track crosses the blue region. LH Io-C and -D emissions are detected in the green regions. In the red regions, the emission frequency generally exceeds 32 MHz. In the dashed boxes, millisecond drifting bursts are observed.

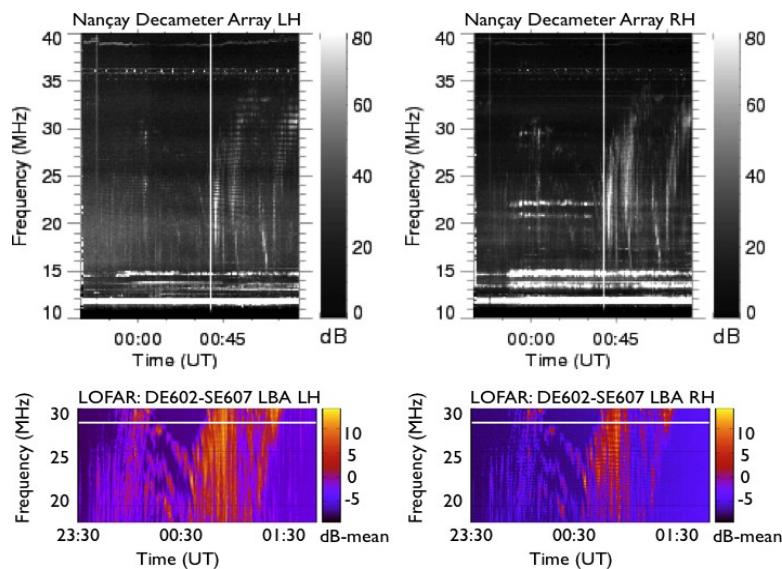


Figure 4 : Commissioning observations (recording raw station voltages) have allowed us to detect Jovian bursts (whose occurrence is predictable) with LOFAR, compare them with Nancay observations, and address the difficulties of low-frequency imaging (disentangling ionospheric fluctuations from source motions). Shown are simultaneous dynamic spectra from the Nancay Decametre Array NDA and from LOFAR, taken on 24 Nov 2011.

## Technical justification

In order to resolve the fast bursts shown in Figure 2, we need high resolution in space and time. Typical burst drift rates are 20 MHz/s, and the individual features extend over  $\sim 1$  MHz corresponding to 50 msec, so that resolutions better than that are required. This is beyond the limits of the correlator output rate. Instead we will record raw voltages in the fly's eye mode for a number of stations with the full resolution (bandwidth  $\times$  integration time=1). Correlations will be done offline with full resolution. We have demonstrated in a number of commissioning experiments (Figure 4 and 5) that this is possible and that we can deal with such data sets.

An optimal combination of resolution in space and time requires about 45 channels per subband with a resolution of 4.5 kHz and 0.22 msec. We will probably use 32 or 64 channels but are also considering to skip the second polyphase filter bank entirely and channelize the data offline with full flexibility. This would not have any impact on the LOFAR resources needed.

According to the models, the motion over 50 msec will be 0.3 arcsec, which corresponds to  $\sim 36$  degrees of phase change on the longest baselines. The signals are so strong that the noise is dominated by self noise (the signal variation itself is stronger than the thermal noise) and the integrated S/N goes with (bandwidth  $\times$  integration time) $^{1/2}$ . Measuring phases to 36 degrees thus requires averaging to 45 kHz and 2.2 msec so that each feature will still be resolved by 20 resolution elements in time and frequency. This is sufficient for the planned analysis. Figure 5 shows that phases can indeed be measured that precisely.

The main difficulty in the analysis consists in the narrowness of individual features which introduces a degeneracy between variations with time and frequency. We are interested in position (phase) changes *with time*. The ionosphere introduces phase changes *with frequency*, which can not be distinguished from the motion a priori. We thus need either external nearby calibrators or (better) several emission regions on Jupiter itself to make differential measurements that are then unaffected by the ionosphere (except for Faraday rotation). We will select observing epochs with expected emissions on both hemispheres to provide this internal calibration. While challenging, our commissioning observations have indicated that this experiment is feasible.

In addition to the raw voltages we are asking to record correlated visibilities with a time resolution of 1 sec in parallel. These additional data will serve as consistency check without increasing the total data volume significantly. Previous experience shows the importance of such tests.

We ask for 3 epochs of 3h each, selected at favourable times of predicted Jovian radio activity (e.g. Table 1). All 8 international stations should be included, as well as the 6 superterp stations. The latter provide additional S/N for external calibrators (much weaker than Jupiter itself). Covering the relevant frequency range 10–40 MHz requires 154 subbands. With this setup the total data rate is about  $(8+6) \times (154/244) \times 6$  Gb/s = 53 Gb/s, well below the maximum output data rate to the storage cluster of 70 Gb/s. Each hour produces a data volume of 24 TB, adding up to a total data volume of 216 TB. No processing at CEP will be required. Instead we ask to transfer the data to the archive directly so that we can download and process them elsewhere. We have local processing and short-term storage capacities at the MPIfR in Bonn, soon also in Nancay and probably in Jülich. The data will be transferred and analysed epoch-by-epoch, which is easily possible with the existing 10 Gb/s link between Jülich and Bonn.

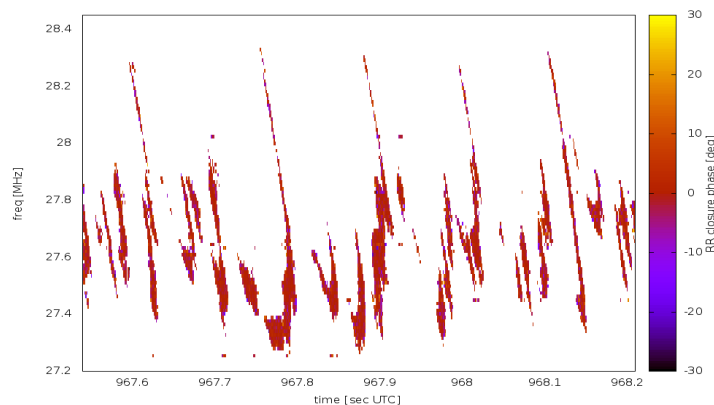


Figure 5 : Closure phase of Io-DAM on the international LOFAR baseline triangle DE602-FR606-RS106 observed on 24/25th November 2011. Areas with low S/N have been blanked. The closure phase does not provide position information, but shows how accurately we can measure phases even with high spectral and temporal resolution. More details and preliminary results of this observation are available at [http://www.astro.uni-bonn.de/~wucknitz/publications/pub.php?2011\\_meudon\\_lofar](http://www.astro.uni-bonn.de/~wucknitz/publications/pub.php?2011_meudon_lofar)

### Supporting observations

We will conduct supporting observations with the Nançay Decameter Array (France, 10–40 MHz) and the Kharkov/UTR-2 array (Ukraine – 8–32 MHz), without capability of imaging but with full polarization measurements (at NDA) and high time and frequency resolutions. These observations will be analyzed jointly with LOFAR observations and provide context, calibrated polarization, etc.

In addition we are planning to observe with the LWA in parallel and correlate the voltages on the very long (ca. 8000 km) baseline. Commissioning observations to test this mode are currently being prepared. LWA time has not been granted for this project yet, but there is a strong interest on their side.

Table 1 : Favourable observation windows in Dec. 2012. The best periods are 7th, 14th and 21<sup>st</sup> Dec 2012 . We can extend this table for any interval of cycle 0. There are generally 1–2 opportunities per month for emission from both hemispheres, and a few more for high probability of emission > 32 MHz.

Date	Start time (UT)	End Time (UT)	Io Emission	Comment
3/12/2012	00:15	04:00	AC	Low probability of emission
5/12/2012	02:00	03:00:00 AM	A	Low elevation
6/12/2012	02:15	03:30	D	Low elevation & Low probability
6/12/2012	19:15	21:30	A then C	Low elevation & C, low prob.
<b>7/12/2012</b>	<b>19:30</b>	<b>21:30</b>	<b>B / D</b>	<b>High probability of emission &gt; 32 MHz</b>
12/12/2012	02:30	04:30	A	Low elevation
13/12/2012	18:45	23:30	A then C	Low elevation & C ,low prob.
<b>14/12/2012</b>	<b>20:45</b>	<b>24:00</b>	<b>B</b>	<b>High probability of emission &gt; 32 MHz</b>
20/12/2012	19:00	24:45	AC	Low elevation & Low probability
<b>21/12/2012</b>	<b>21:00</b>	<b>24:30</b>	<b>B</b>	<b>High probability of emission &gt; 32 MHz</b>
27/12/2012	19:45	24:30	AC	Low elevation & Low probability
28/12/2012	21:30	24:45	B	Max probability before 22:30
30/12/2012	21:30	23:00	D	Low probability

### Co-Is and role

Name	Affiliation	Status	Expertise	Role in this proposal	% FTE
Olaf Wucknitz	MPIfR Bonn	P.I. of LBG	LOFAR LB data analysis	coordination, LB data analysis	5-10
Philippe Zarka	LESIA, CNRS-Obs. Paris	P.I. of Planets/Exoplanets WG	Nançay BF data analysis, LOFAR BF commissioning (Jupiter/Saturn), polarization	coordination, data analysis (incl. Nançay observations)	10
Julien Girard	LESIA, CNRS-Obs. Paris	PEWGW associate member	LOFAR IM commissioning (Jupiter), beyond standard imaging	LOFAR LB data analysis	10
Sébastien Hess	LATMOS/IPSL, Guyancourt	PEWGW member	theoretical predictions & modelling, LOFAR IM commissioning (Jupiter)	theoretical predictions & modelling/interpretation	5-10
Imke de Pater	Univ. Berkeley	PEWGW member	Jupiter synchrotron imaging	data analysis	10
Laurent Lamy	LESIA, CNRS-Obs. Paris	-	Planetology/plasmas, spacecraft (Cassini) BF data	data analysis	10
Vladimir Ryabov	Future Univ. Hakodate	-	UTR-2 observations & BF data analysis, exoplanet search	data analysis	10
Alexander Konovalev	IRA, Kharkov	-	UTR-2 (Leader) observations & BF data analysis	Supporting observations at UTR-2 (10-32 MHz)	10
James Anderson	MPIfR Bonn		LB expertise		

### References

Dulk, G. A., *Astrophys. J.*, 159, 671-684, 1970 ; Hess, S., P. Zarka, and F. Mottez, *Planet. Space Sci.*, 55, 89-99, 2007 ; Hess, S., et al., *Planet. Space Sci.*, 57, 23–33, 2009 ; Hess, S., et al., *Planet. Space Sci.*, 58, 1188-1198, 2010; Ladreiter, H. P., P. Zarka, and A. Lecacheux, *Planet. Space Sci.*, 42, 919-931, 1994 ; Nigl, A., et al., *Astron. Astrophys.*, 471, 1099–1104, 2007 ; Treumann, R., *Astron. Astrophys. Rev.*, 13, 229–315, 2006 ; Zarka, P., *J. Geophys. Res.*, 103, 20159-20194, 1998 ; Zarka, P., *Planet. Space Sci.*, 52, 1455-1467, 2004a ; Zarka, P., *Adv. Space Res.*, 33 (11), 2045-2060, 2004b